Retinal function in advanced multiple sclerosis

Supplementary Materials

James V. M. Hanson, Sara Single, Rahel B. Eberle, Veronika Kana, Benjamin V. Ineichen, Christina Gerth-Kahlert

Supplementary Methods

ERG (electroretinography)

Mydriasis was accomplished with topical application of 0.5% tropicamide and 5% phenylephrine, with 0.4% oxybuprocaine being instilled prior to positioning the Dawson-Trick-Litzkow (DTL) electrodes. All recordings were made by a single experienced electrophysiologist (author JVMH) whilst ensuring that the DTL threads were positioned horizontally at the lower lid margin to ensure consistency.[1, 2]

After a 20 minute period of dark adaptation, subjects were presented with 0.01cd/m^2 flashes ('DA 0.01') followed by 3.0cd/m^2 flashes ('DA 3.0'). Following these measurements, subjects were adapted to a rod-bleaching 30cd/m^2 light for 10 minutes before being presented with 3.0cd/m^2 stimuli, both flickering (30Hz frequency; 'flicker') and single flashes ('LA 3.0') against a 30cd/m^2 background. All stimuli were presented via a full-field stimulator with diffusor, of 4ms duration, and composed of white light. Multiple responses were recorded for each condition to verify reproducibility, which were then averaged. Recordings were made with a bandwidth of 0.3 – 300 Hz and a sampling rate of 2 kHz, permitting a temporal resolution of 0.5ms.

OCT (optical coherence tomography)

All OCT scans were acquired using a Spectralis device (Heidelberg Engineering, Heidelberg, Germany) using manufacturer's protocols. The centre of the opening of Bruch's membrane at the optic nerve head and the centre of the foveal pit were both defined using the Anatomic Position System (APS) contained within the software. 24 radially oriented line scans separated by 15º were performed, seamlessly followed by three circumpapillary scans of 3.5mm, 4.1mm, and 4.7mm (approximately 12º, 14º, and 16º,

respectively). Automatic Real-time Tracking (ART) averaging was ≥25 for each radial or circular scan. Volume scans (30° vertical by 15° horizontal, 19 vertically oriented sections separated by 240µm, 25 ART) were centred on the fovea. All OCT scans were performed in HR (high resolution) mode. Post-hoc quality verification[3] and processing were performed as previously described.[4, 5] Each of the macular OCT parameters (ganglion cell-inner plexiform complex, GCIP; inner nuclear layer, INL; outer plexiform layer, OPL; outer nuclear layer, ONL; outer retinal layers, ORL) was quantified as the volume (in mm^3) of each layer or complex measured over a 3.45mm diameter circle. RNFL thickness measurements were obtained from the 3.5mm circumpapillary scan; the global thickness (RNFL-G), averaged from all sectoral measurements, was analyzed, along with thickness in the temporal (RNFL-T) and papillomacular bundle (RNFL-PMB) sectors. Post-hoc analysis included verifying that the OCT images were of sufficient quality, as defined by the OSCAR-IB criteria,[3] and discarding any unacceptable scans. Following this step, the volume scans were automatically segmented, followed by manual verification and correction when necessary, using proprietary software (Heidelberg Engineering). This enabled visualization and quantification of the macular ganglion cell-inner plexiform layer complex (GCIP), inner nuclear layer (INL), outer plexiform layer (OPL), outer nuclear layer (ONL), and outer retinal layers (ORL; defined proximally by the external limiting membrane [ELM] and distally by Bruch's membrane [BM], and therefore comprising mainly the photoreceptors) for each eye. All OCT scans were acquired and verified by a single experienced operator (JVMH).

Statistical Analyses

In addition to the group comparisons of ERG findings and analyses of the effects of MS on selected ERG outcomes described in the main text, we also used generalized estimating equation (GEE) models adjusted for age and sex to compare the following OCT parameters in MS +ON, MS –ON, and HC eyes: RNFL-G; RNFL-T; RNFL-PMB; GCIP; INL; OPL; ONL; ORL.

Prior to data collection, we chose DA 3.0 and LA 3.0 b-wave peak times as the most appropriate variables for detailed analysis of the effects of disability (as quantified by the Expanded Disability Status Scale [EDSS] score), disease duration, ON history, MS subtype and treatment status, disease status, and treatment, based on the results of previously published manuscripts. We present a summary of the results of all relevant cross-sectional studies, both recent and historical, in Supplementary Table 1 below. For context, the first published recommended standards for ERG recording were published in

1989,[6] and lack of standardization precludes meaningful comparison of ERG findings recorded with varying protocols before then. In particular, the majority of studies published before the introduction of recommended standards did not present any analysis of ERG peak times. Similarly, current MS phenotypical classifications[7] and quantification of EDSS[8] are relatively recent developments, and comparisons of disease MS characteristics between older studies, and with newer work, is challenging.

For the statistical analyses, the following R packages were used in addition to base packages: *visda*t to assess the pattern of missing data,[9] *missForest* o impute missing data,[10] *geepack* to fit the generalised estimating equation (GEE) models,[11] *table1* and *kableExtra* to create tables of descriptive statistics and print them in LaTeX,[12, 13] *tableone* to create the tables of baseline characteristics (main text, Table XX),[14] *xtable* to generate LaTeX tables,[15] *biostatUZH* to format the p-values and GEE output table,[16] *broom*, *tidyverse* and *dplyr* to tidy data and model outputs,[17-19] *ggplot2* to make plots,[20] and *ggpubr* to arrange the graphs.[21]

Supplementary Results

A number of individual eyes were completely excluded from analysis due to strabismus and/or amblyopia (potentially making it more difficult to detect previous ON; MS: n=6), previous uveitis (MS: n=1), asymptomatic epiretinal membrane precluding accurate segmentation of macular OCT scans (HC: n=2), presumed congenital optic disc anomaly (MS: n=1), early-stage macular degeneration (MS: n=1), history of retinal surgery (MS: n=1),) and OCT and visual acuity findings ambiguous with regard to previous subclinical ON (HC: n=1) .

In addition to these exclusions of data at the eye level, individual parameters were not recorded and/or analyzed in small numbers of subjects or eyes. For example, tremor prevented acquisition of OCT scans of sufficient quality in two people with MS (pwMS); photophobia/discomfort during 30Hz stimulation prevented the recording of usable flicker ERG responses in one subject with MS and one HC; it was not possible to record macular OCT volume scans in two MS eyes due to loss of central vision and fixation after severe ON; radiological disease activity could not be ascertained in a single subject with MS due to a recently implanted medical device; pupil dilation (and therefore ERG recording) was not possible in one eye of a single HC subject with previous iris trauma following cataract surgery; and RNFL values

were not suitable for analysis in one eye of one subject with MS and both eyes of one HC subject due to peri-papillary atrophy. Microcystic macular oedema (MMO) was not visible in any of the eyes analysed.

Descriptive statistics for the OCT results are provided in Supplementary Table 2 (including the number of missing/imputed data for each condition) and illustrated in Supplementary Figure 1, with the results of the GEE provided in Supplementary Table 3. We found very strong evidence of thinner RNFL-G, RNFL-T, RNFL-PMB, and GCIP in MS +ON and MS -ON eyes compared to HC (Supplementary Table 3). Although we did not compare MS+ON and MS-ON groups directly, the estimates of each coefficient were approximately twice as great in MS+ON eyes, consistent with greater inner retinal thinning in eyes with previous ON. We also recorded moderate evidence of INL thickening in MS+ON eyes relative to HC eyes ($p=0.013$). We did not find any evidence of inter-group differences in any other OCT parameters.

To verify the robustness of our group comparisons, we plotted estimated coefficients and 95% CI for the imputed MS dataset used for analysis and for the complete case MS dataset (i.e., without imputation). No appreciable differences between the estimates were observed, suggesting that our findings were unaffected by imputation and are therefore robust (data not shown).

Supplementary Discussion

Our OCT findings are consistent with those previously published by other authors, for example as meta-analyzed by Petzold and colleagues,[22] namely inner retinal thinning in eyes of pwMS both with and (to a lesser extent) without previous ON relative to HC subjects. The moderate evidence of INL thickening in MS +ON eyes is also compatible with previous literature (e.g. [22-24]). The fact that previous ON was found to have no effect on the ERG parameters analyzed in the present study suggests that this INL thickening is unlikely to affect bipolar cell function. The INL also contains the nuclei of amacrine cells and Müller glia in addition to those of bipolar cells, and other authors have proposed that INL thickening after ON is likely to be mediated by Müller cell pathology.[23] Our data are compatible with this hypothesis.

Study	N (eyes)§	MS type	EDSS	DD	ON	ERG AMP	ERG PEAK	Notes
Coupland 1982 [25]	105 (210)	NA	NA	NA	128/210	NA	NA A Delayed B	Only b-wave peak times analyzed
Feinsod 1971 [26]	8 (16)	NA	NA	NA	NA	Increased A (5/16 eyes) Reduced A (2/16 eyes) Increased B (12/16 eyes) Reduced B (2/16 eyes) Otherwise normal	NA	All patients had optic atrophy and reduced or non-recordable VEP, unclear if uni- or bilateral
Feinsod 1973 [27]	35 (70)	NA	NA	NA	NA	Increased A (11/70 eyes) Reduced A (21/70 eyes) Increased B (17/70 eyes) Reduced B (27/70 eyes) Otherwise normal	NA	Patients categorized as having had 'visual symptoms' or not, but not specifically as having had ON
Forooghian 2006 [28]	34 (68)	RRMS (21) SPMS (10) PPMS (3)	2.9*	90.0*	≥17/68 (see notes)	Normal (see notes)	Delayed DA3.0B Delayed LA3.0B Otherwise normal	Precise number of ON eyes not given. Non-standard rod a-wave also delayed; OP amplitude sum reduced.
Forooghian 2007 [29]	34 (68)	NA	2.9*	NA	NA	Normal (see notes)	Delayed DA3.0B Otherwise normal (see notes)	Significance <0.01 to control for multiplicity; other (unspecified) ERG parameters also abnormal
Fraser 2011 [30]	27 (54)	RRMS (27)	NA	NA	27/54	Normal	NA	Study primarily of unilateral ON, MS patients included
Gills 1966 [31]	27 (54)	NA	NA	108*	NA	Reduced	NA	Patients with 'advanced' MS; 'majority' with pale/atrophic ONH
Gorczyca 2004 [32]	28 (NA)	RRMS (28)	NA	NA	NA	Normal Reduced (see notes)	NA	ERG data not shown in detail; data likely incomplete; 'reduced' in 2 patients with high antibody titers, otherwise normal
Gundogan 2007 [33]	39 (39)	RRMS (35) SPMS (4)	NA	64.8*	0/39	Normal	Delayed DA0.01B DelayedDA3.0A Delayed DA3.0B Otherwise normal	
Hamurcu 2017 [34]	51 (??)	NA	NA	NA	22/51 patients	Normal Rod Reduced Flicker Reduced Cone (see notes)	Delayed Cone	Data presented incompletely in table; text and table contradictory with regard to differences between MS patients with and without previous ON
Hanson 2018 [4]	32 (61)	CIS (11) RRMS (19)	1.0 (0.0-4.0)	18.5	23/61†	Increased DA0.01B‡ Increased DA3.0A‡	Delayed DA3.0A‡ Delayed Flicker‡	

		PPMS (2)				Otherwise normal‡	Delayed LA3.0A‡ Delayed LA3.0B‡ Otherwise normal‡	
Ikeda 1978 [35]	60 (120)	NA	NA	NA	93/120	Normal Reduced (see notes)	NA	ON cohort not analyzed as a whole - patients categorized based on VEP and ERG results.
Papakostopoulos 1989 [36]	14 (28)	NA	NA	43.7*	14/28	Normal A Reduced B	NA	5/14 patients examined within 3/12 of ON. ERG reduced only in ON eyes. Peak times not analyzed (36.5 MS ON vs. 35.5 MS vs. 34.4ms normal)
Persson 1984 [37]	15 (30)	NA	NA	NA	12/30	Normal	NA	Only 1 stimulus condition (after 5 minutes dark adaptation)
Pierelli 1985 [38]	15 (30)	NA	NA	NA	22/30	NA A Increased B	NA A Normal B	Only photopic b-waves analyzed
Shushtarian 2017 [39]	30 (30)	NA	NA	NA	NA	Normal B	Delayed B	Only b-waves analyzed, for one stimulation type only.
Sriram 2014 [40]	58 (58)	RRMS (58)	NA	56.4*	0/58	Normal	Delayed LA3.0B Otherwise normal	
You 2018 [41]	77 (77)	RRMS (77)	1.0 (0.0-6.0)	48.0	0/77	Normal	Delayed DA3.0A Delayed LA3.0B Otherwise normal	
You 2019 [42]	131 (262)	RRMS (131)	1.0 (0.0-6.0)	48.0	64/262†	Normal	Delayed DA3.0A Delayed Flicker Delayed LA3.0B Otherwise normal	

Supplementary Table 1. Summary of previously published electroretinogram (ERG) findings in individuals with multiple sclerosis (MS). For ease of interpretation, subnormal findings are shown in red text, supernormal in green text, and normal findings in black text. AMP, amplitude (of ERG); CIS, clinically isolated syndrome; DD, disease duration (in months); EDSS, Expanded Disability Status Scale score (median and range provided unless otherwise indicated); ERG, electroretinogram; MS, multiple sclerosis; NA, not available; ON, optic neuritis; PEAK, peak time (of ERG); PPMS, primary progressive multiple sclerosis; RRMS, relapsing-remitting multiple sclerosis; SPMS, secondary progressive multiple sclerosis. *denotes mean, otherwise median. †in analyses, ON was found not to influence the results. ‡at $p<0.05$, as in the majority of published studies (note that not all studies provided details of correction for multiple hypothesis testing). §MS patients only (some studies also included patients with conditions other than MS)

	HC	MS -ON	MS +ON
N eyes	73	67	35
RNFL.G			
Mean (SD)	102.0 (8.8)	91.2 (10.1)	78.1 (16.4)
Median [IQR]	103.0 [11.0]	91.0 [13.3]	81.0 [16.0]
Missing (%)	2 (2.7)	5 (7.5)	2 (5.7)
RNFL.T			
Mean (SD)	68.8 (9.6)	58.0 (10.7)	43.8 (13.9)
Median [IQR]	69.0 [12.0]	57.5 [16.0]	45.0 [19.0]
Missing (%)	2 (2.7)	5 (7.5)	2 (5.7)
RNFL.PMB			
Mean (SD)	53.4 (7.6)	44.6 (8.8)	34.7 (10.9)
Median [IQR]	53.0 [11.0]	45.0 [12.0]	32.0 [15.0]
Missing (%)	3 (4.1)	5 (7.5)	2 (5.7)
GCIP			
Mean (SD)	0.81 (0.1)	0.71 (0.10)	0.59 (0.1)
Median [IQR]	0.81 [0.1]	0.71 [0.1]	0.59 [0.2]
Missing (%)	0 (0.0)	5 (7.5)	4 (11.4)
INL			
Mean (SD)	0.39 (0.0)	0.39 (0.0)	0.40 (0.0)
Median [IQR]	0.38 [0.0]	0.39 [0.0]	0.40 [0.1]
Missing (%)	0 (0.0)	5 (7.5)	4 (11.4)
OPL			
Mean (SD)	0.27 (0.0)	0.27 (0 0)	0.27 (0.0)
Median [IQR]	0.26 [0.0]	0.26 [0.0]	0.27 [0.0]
Missing (%)	0 (0.0)	5 (7.5)	4 (11.4)
ONL			
Mean (SD)	0.69 (0.1)	0.68 (0.1)	0.68 (0.1)
Median [IQR]	0.67 [0.1]	0.68 [0.1]	0.68 [0.2]
Missing (%)	0 (0.0)	5 (7.5)	4 (11.4)
ORL			
Mean (SD)	0.76 (0.0)	0.76 (0.0)	0.77 (0.0)
Median [IQR]	0.77 [0.0]	0.76 [0.0]	0.76 [0.0]
Missing (%)	0 (0.0)	5 (7.5)	4 (11.4)

Supplementary Table 2 (previous page). Descriptive statistics of optical coherence tomography (OCT) results in the study cohort. GCIP, ganglion cell-inner plexiform layer complex; HC, healthy control; INL, inner nuclear layer; IQR, inter-quartile range; MS, multiple sclerosis; ON, optic neuritis; ONL, outer nuclear layer; OPL, outer plexiform layer; ORL, outer retinal layers; RNFL.G, retinal nerve fiber layer (global average); RNFL.PMB, retinal nerve fiber layer (papillomacular bundle); RNFL.T, retinal nerve fiber layer (temporal quadrant); SD, standard deviation. RNFL.G, .T, and .PMB are quantified as thickness in microns (μm), with all other measures being expressed as volume in mm^3.

Variable	Coefficient	Estimate	SE	95% CI	p-value
RNFL.G	HC (Intercept)	106.93	4.26	98.58 to 115.28	
	MS -ON	-10.90	1.95	-14.71 to -7.08	**< 0.0001**
	MS +ON	-23.03	2.97	-28.86 to -17.2	**< 0.0001**
RNFL.T	HC (Intercept)	66.10	4.46	57.35 to 74.85	
	MS -ON	-10.83	1.98	-14.71 to -6.96	**< 0.0001**
	MS +ON	-22.59	2.51	-27.51 to -17.68	**< 0.0001**
RNFL.PMB	HC (Intercept)	51.12	3.88	43.52 to 58.73	
	MS -ON	-9.02	1.64	-12.23 to -5.81	**< 0.0001**
	MS +ON	-16.51	2.07	-20.58 to -12.45	**< 0.0001**
GCIP	HC (Intercept)	0.85	0.04	0.78 to 0.93	
	MS -ON	-0.10	0.02	-0.13 to -0.07	**< 0.0001**
	MS +ON	-0.20	0.02	-0.25 to -0.16	**< 0.0001**
INL	HC (Intercept)	0.39	0.01	0.36 to 0.41	
	MS -ON	0.00	0.01	-0.01 to 0.01	0.81
	MS +ON	0.02	0.01	0.00 to 0.03	**0.013**
OPL	HC (Intercept)	0.26	0.01	0.24 to 0.29	
	MS -ON	0.00	0.01	-0.01 to 0.02	0.72
	MS +ON	0.00	0.01	-0.01 to 0.02	0.66
ONL	HC (Intercept)	0.71	0.03	0.65 to 0.78	
	MS -ON	-0.02	0.01	-0.05 to 0.01	0.43
	MS +ON	-0.01	0.02	-0.04 to 0.02	0.72
ORL	HC (Intercept)	0.77	0.01	0.75 to 0.79	
	MS -ON	0.00	0.00	-0.01 to 0.01	0.90
	MS +ON	0.00	0.01	-0.01 to 0.01	0.95

Supplementary Table 3. Results of generalised estimating equation (GEE) models adjusted for age and sex comparing optical coherence tomography (OCT) results in eyes of people with multiple sclerosis both with (MS +ON) and without (MS –ON) previous optic neuritis with those of healthy control subjects. CI, confidence interval; GCIP, ganglion cell-inner plexiform layer complex; HC, healthy control; INL, inner nuclear layer; IQR, inter-quartile range; MS, multiple sclerosis; ON, optic neuritis; ONL, outer nuclear layer; OPL, outer plexiform layer; ORL, outer retinal layers; RNFL.G, retinal nerve fiber layer (global average); RNFL.PMB, retinal nerve fiber layer (papillomacular bundle); RNFL.T, retinal nerve fiber layer (temporal quadrant); SD, standard deviation; SE, standard error. RNFL.G, .T, and .PMB are quantified as thickness in microns (μm), with all other measures being expressed as volume in mm^3. Corrected p-values representing moderate, strong, or very strong evidence of a difference between the relevant MS subgroup and HC cohort are highlighted in bold (more details available in the 'Statistical Analysis' subsection in the main text).

Variable	Coefficient	Estimate	SE	95% CI
DA3.0b.PEAK	RRMS (intercept)	52.13	2.27	47.68 to 56.58
	SPMS	-0.44	1.01	-2.41 to 1.53
	PPMS	-1.66	1.39	-4.38 to 1.05
	Active CLI (No) (intercept)	52.94	2.12	48.78 to 57.1
	Active CLI (Yes)	-0.53	1.70	-3.85 to 2.8
	Active RAD (No) (intercept)	52.79	2.12	48.63 to 56.95
	Active RAD (Yes)	0.04	1.50	-2.9 to 2.99
	PROG (No) (intercept)	51.69	2.43	46.93 to 56.45
	PROG (Yes)	-2.08	1.11	-4.26 to 0.09
LA3.0b.PEAK	RRMS (intercept)	28.08	0.76	26.59 to 29.58
	SPMS	-0.09	0.39	-0.85 to 0.66
	PPMS	-0.37	0.50	-1.35 to 0.62
	Active CLI (No) (intercept)	28.27	0.77	26.76 to 29.78
	Active CLI (Yes)	-0.16	0.73	-1.6 to 1.28
	Active RAD (No) (intercept)	28.43	0.75	26.95 to 29.9
	Active RAD (Yes)	-0.39	0.49	-1.35 to 0.58
	PROG (No) (intercept)	28.18	0.76	26.68 to 29.67
	PROG (Yes)	-0.09	0.37	-0.81 to 0.64

Supplementary Table 4. Results of exploratory generalized estimating equation (GEE) models adjusted for age and sex examining the influence of multiple sclerosis (MS) phenotype and clinical status on selected electroretinogram (ERG) outcome measures. For each model, the intercept is the expected value with all predictors as zero, with the estimate quantifying the expected change to the intercept when switching MS category or changing MS clinical statuses from 'no' to 'yes', respectively, with all other factors remaining constant. CI, confidence interval; CLI, clinically (active); DA, dark-adapted; LA, light-adapted; PEAK, peak time; PPMS, primary progressive multiple sclerosis; PROG, progression; RAD, radiologically (active); RRMS, relapsing-remitting multiple sclerosis; SE, standard error; SPMS, secondary progressive multiple sclerosis

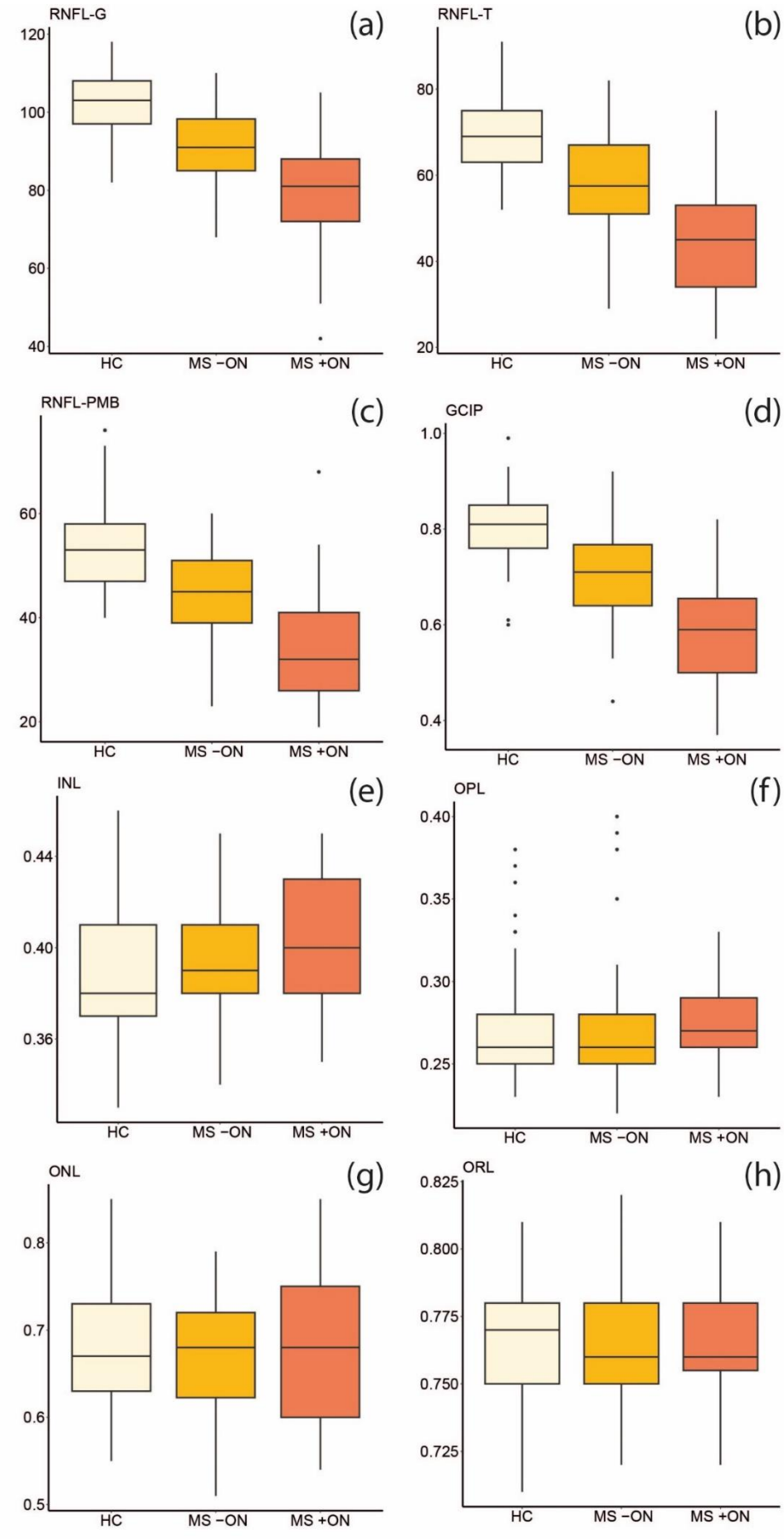
RNFL-G
(a)
120
100
80
60
40
HC
MS −ON
MS +ON
RNFL-T
(b)
80
60
40
20
HC
MS −ON
MS +ON
RNFL-PMB
(c)
60
40
20
HC
MS −ON
MS +ON
GCIP
(d)
1.0
0.8
0.6
0.4
HC
MS −ON
MS +ON
INL
(e)
0.44
0.40
0.36
HC
MS −ON
MS +ON
OPL
(f)
0.40
0.35
0.30
0.25
HC
MS −ON
MS +ON
ONL
(g)
0.8
0.7
0.6
0.5
HC
MS −ON
MS +ON
ORL
(h)
0.825
0.800
0.775
0.750
0.725
HC
MS −ON
MS +ON

Supplementary Figure 1 (a-h; previous page). Boxplots showing optical coherence tomography (OCT) results in eyes of people with multiple sclerosis both with (MS +ON) and without (MS –ON) previous optic neuritis with those of healthy control (HC) subjects. Y-axes show thickness in microns (a-c) and volume in mm3 (d-h). Median values and interquartile ranges are indicated by horizontal lines and boxes, respectively; whiskers show the lowest and highest data points still within 1.5 IQR of the lower and upper quartiles. Individual outlying data points are represented by black dots. IGCIP, ganglion cell-inner plexiform layer complex; HC, healthy control; INL, inner nuclear layer; MS, multiple sclerosis; ON, optic neuritis; ONL, outer nuclear layer; OPL, outer plexiform layer; ORL, outer retinal layers; RNFL-G, retinal nerve fiber layer (global average); RNFL-PMB, retinal nerve fiber layer (papillomacular bundle); RNFL-T, retinal nerve fiber layer (temporal quadrant).

Supplementary References

1. Brouwer AH, de Wit GC, de Boer JH and van Genderen MM. Effects of DTL electrode position on the amplitude and implicit time of the electroretinogram. *Documenta Ophthalmologica* 2020; 140: 201-209. DOI: 10.1007/s10633-019-09733-3.
2. Kurtenbach A, Kramer S, Strasser T, et al. The importance of electrode position in visual electrophysiology. *Doc Ophthalmol* 2017; 134: 129-134. 2017/02/23. DOI: 10.1007/s10633-017-9579-9.
3. Schippling S, Balk LJ, Costello F, et al. Quality control for retinal OCT in multiple sclerosis: validation of the OSCAR-IB criteria. *Mult Scler* 2015; 21: 163-170. 2014/06/21. DOI: 10.1177/1352458514538110.
4. Hanson JVM, Hediger M, Manogaran P, et al. Outer Retinal Dysfunction in the Absence of Structural Abnormalities in Multiple Sclerosis. *Invest Ophthalmol Vis Sci* 2018; 59: 549-560. 2018/01/27. DOI: 10.1167/iovs.17-22821.
5. Hanson JVM, Ng M-Y, Hayward-Koennecke HK, et al. A three-year longitudinal study of retinal function and structure in patients with multiple sclerosis. *Documenta Ophthalmologica* 2022; 144: 3-16. DOI: 10.1007/s10633-021-09855-7.
6. Marmor MF, Arden GB, Nilsson SEG and Zrenner E. Standard for Clinical Electroretinography: International Standardization Committee. *Archives of Ophthalmology* 1989; 107: 816-819. DOI: 10.1001/archopht.1989.01070010838024.
7. Lublin FD, Reingold SC and Sclerosis* NMSSACoCToNAiM. Defining the clinical course of multiple sclerosis. *Results of an international survey* 1996; 46: 907-911. DOI: 10.1212/wnl.46.4.907.
8. Kurtzke JF. Rating neurologic impairment in multiple sclerosis: an expanded disability status scale (EDSS). *Neurology* 1983; 33: 1444-1452. DOI: 10.1212/wnl.33.11.1444.
9. Tierney N. visdat: Visualising whole data frames. *The Journal of Open Source Software* 2017; 2: 355.
10. Stekhoven DJ and Bühlmann P. MissForest--non-parametric missing value imputation for mixed-type data. *Bioinformatics* 2012; 28: 112-118. 20111028. DOI: 10.1093/bioinformatics/btr597.
11. Højsgaard S, Halekoh U and Yan J. The R Package geepack for Generalized Estimating Equations. *Journal of Statistical Software* 2005; 15: 1 - 11. DOI: 10.18637/jss.v015.i02.
12. Rich B. table1: Tables of Descriptive Statistics in HTML. R package version 1.4.3 ed. 2023.
13. Zhu K. kableExtra: Construct complex table with 'kable' and Pipe Syntax. 2021.
14. Yoshida K and Bartel A. tableone: Create 'Table 1' to Describe Baseline Characteristics with or without Propensity Score Weights. 2022.
15. Dahl DB, Scott D, Roosen C, et al. xtable: Export Tables to LaTeX or HTML. 2019.
16. Held L, Gerber F, Rufibach K, et al. biostatUZH: Misc Tools of the Department of Biostatistics, EBPI, University of Zurich. 2022.
17. Robinson D, Hayes A and Couch S. broom: Convert Statistical Objects into Tidy Tibbles. 2023.
18. Wickham H, Averick M, Bryan J, et al. Welcome to the Tidyverse. *The Journal of Open Source Software* 2019; 4: 1686. DOI: https://doi.org/10.21105/joss.01686.
19. Wickham H, Francois R, Henry L and Müller K. dyplyr: A Grammar of Data Manipulation. 2022.
20. Wickham H. *ggplot2: Elegant Graphics for Data Analysis*. 2 ed. New York: Springer, 2016.

21. Kassambara A. ggpubr: 'ggplot2' Based Publication Ready Plots. R package version 0.5.0 ed. 2022.
22. Petzold A, Balcer LJ, Calabresi PA, et al. Retinal layer segmentation in multiple sclerosis: a systematic review and meta-analysis. *Lancet Neurol* 2017; 16: 797-812. 2017/09/19. DOI: 10.1016/s1474-4422(17)30278-8.
23. Balk LJ, Coric D, Knier B, et al. Retinal inner nuclear layer volume reflects inflammatory disease activity in multiple sclerosis; a longitudinal OCT study. *Multiple sclerosis journal - experimental, translational and clinical* 2019; 5: 2055217319871582. 2019/09/17. DOI: 10.1177/2055217319871582.
24. Wicki CA, Manogaran P, Simic T, et al. Bilateral retinal pathology following a first-ever clinical episode of autoimmune optic neuritis. *Neurol Neuroimmunol Neuroinflamm* 2020; 7 2020/01/24. DOI: 10.1212/nxi.0000000000000671.
25. Coupland SG and Kirkham TH. Flash electroretinogram abnormalities in patients with clinically definite multiple sclerosis. *Can J Neurol Sci* 1982; 9: 325-330. 1982/08/01.
26. Feinsod M, Rowe H and Auerbach E. Changes in the electroretinogram in patients with optic nerve lesions. *Doc Ophthalmol* 1971; 29: 169-200. 1971/05/14.
27. Feinsod M, Abramsky O and Auerbach E. Electrophysiological examinations of the visual system in multiple sclerosis. *Journal of the Neurological Sciences* 1973; 20: 161-175. DOI: https://doi.org/10.1016/0022-510X(73)90028-2.
28. Forooghian F, Sproule M, Westall C, et al. Electroretinographic abnormalities in multiple sclerosis: possible role for retinal autoantibodies. *Doc Ophthalmol* 2006; 113: 123-132. DOI: 10.1007/s10633-006-9022-0.
29. Forooghian F, Adamus G, Sproule M, et al. Enolase autoantibodies and retinal function in multiple sclerosis patients. *Graefes Arch Clin Exp Ophthalmol* 2007; 245: 1077-1084. 2007/01/16. DOI: 10.1007/s00417-006-0527-8.
30. Fraser CL and Holder GE. Electroretinogram findings in unilateral optic neuritis. *Doc Ophthalmol* 2011; 123: 173-178. DOI: 10.1007/s10633-011-9294-x.
31. Gills JP, Jr. Electroretinographic abnormalities and advanced multiple sclerosis. *Invest Ophthalmol* 1966; 5: 555-559. 1966/12/01.
32. Gorczyca WA, Ejma M, Witkowska D, et al. Retinal Antigens Are Recognized by Antibodies Present in Sera of Patients with Multiple Sclerosis. *Ophthalmic Research* 2004; 36: 120-123. DOI: 10.1159/000076892.
33. Gundogan FC, Demirkaya S and Sobaci G. Is optical coherence tomography really a new biomarker candidate in multiple sclerosis?--A structural and functional evaluation. *Invest Ophthalmol Vis Sci* 2007; 48: 5773-5781. 2007/12/07. DOI: 10.1167/iovs.07-0834.
34. Hamurcu M, Orhan G, Sarıcaoğlu MS, et al. Analysis of multiple sclerosis patients with electrophysiological and structural tests. *Int Ophthalmol* 2017; 37: 649-653. 2016/08/20. DOI: 10.1007/s10792-016-0324-2.
35. Ikeda H, Tremain KE and Sanders MD. Neurophysiological investigation in optic nerve disease: combined assessment of the visual evoked response and electroretinogram. *Br J Ophthalmol* 1978; 62: 227-239. 1978/04/01.
36. Papakostopoulos D, Fotiou F, Hart JC and Banerji NK. The electroretinogram in multiple sclerosis and demyelinating optic neuritis. *Electroencephalogr Clin Neurophysiol* 1989; 74: 1-10. 1989/01/01.
37. Persson HE and Wanger P. Pattern-reversal electroretinograms and visual evoked cortical potentials in multiple sclerosis. *Br J Ophthalmol* 1984; 68: 760-764. 1984/10/01.
38. Pierelli F, Pozzessere G, Stefano E, et al. Pattern visual evoked potentials and flash electroretinogram in clinically definite multiple sclerosis. *European neurology* 1985; 24: 324-329. 1985/01/01.
39. Shushtarian SMM, Adhami-Moghadam F and Naser M. Electroretinographic Changes in Multiple Sclerosis Patients with Abnormal Visual Evoked Potentials. *Journal of Ophthalmic and Optometric Sciences* 2018; 1: 34-38. DOI: 10.22037/joos.v1i3.22729.
40. Sriram P, Wang C, Yiannikas C, et al. Relationship between optical coherence tomography and electrophysiology of the visual pathway in non-optic neuritis eyes of multiple sclerosis patients. *PLoS One* 2014; 9: e102546. 2014/08/29. DOI: 10.1371/journal.pone.0102546.
41. You Y, Graham EC, Shen T, et al. Progressive inner nuclear layer dysfunction in non-optic neuritis eyes in MS. *Neurol Neuroimmunol Neuroinflamm* 2018; 5: e427. 2017/12/21. DOI: 10.1212/nxi.0000000000000427.
42. You Y, Zhu L, Zhang T, et al. Evidence of Muller Glial Dysfunction in Patients with Aquaporin-4 Immunoglobulin G-Positive Neuromyelitis Optica Spectrum Disorder. *Ophthalmology* 2019; 126: 801-810. 2019/02/04. DOI: 10.1016/j.ophtha.2019.01.016.